

Flapping Wing Aerial Vehicle

A Final Year Project Report

Presented to

SCHOOL OF MECHANICAL & MANUFACTURING ENGINEERING

Department of Mechanical Engineering

NUST

ISLAMABAD, PAKISTAN

In Partial Fulfillment

of the Requirements for the Degree of

Bachelor of Mechanical Engineering

by

Feroze Sharjeel

Toheed Ahmad

Ans Sadiq

Ahad Ali Meer

June 2023

EXAMINATION COMMITTEE

We hereby recommend that the final year project report prepared under our supervision by:

Feroze Sharjeel 290744.
Toheed Ahmad 283594
Ans Sadiq . 294916
Ahad Ali Meer 298050.

Titled: “Flapping Wing Aerial Vehicle” be accepted in partial fulfillment of the requirements for the award of Bachelor of Mechanical Engineering degree with grade ____

Supervisor: Dr. Emad Uddin, Head of Department SMME National University of Sciences and Technology (NUST)	_____ Dated:
Committee Member: Dr. Jawad Khan, Assistant Professor SMME National University of Sciences and Technology (NUST)	_____ Dated:
Committee Member: Dr. Zaib, Assistant Professor SMME National University of Sciences and Technology (NUST)	_____ Dated:

(Head of Department)

(Date)

COUNTERSIGNED

Dated: _____

Principal _____

ABSTRACT

This report describes the design, implementation, and testing of a Flapping Wing Aerial Vehicle (FWAV) prototype, which was inspired by the flight mechanism of birds and insects. The FWAV's design offers improved maneuverability and agility compared to traditional aircraft, making it a potential alternative for specific applications.

The design process involved aerodynamic analysis, material selection, and component integration. The FWAV prototype was equipped with a microcontroller-based control system that allowed for stable and precise flight control. The prototype underwent extensive testing, demonstrating its capability for stable hovering, forward flight, and turning maneuvers.

This project's outcomes offer valuable insights into the design and implementation of a flapping wing aerial vehicle, which has potential applications in various fields such as surveillance, environmental monitoring, and search and rescue operations. The FWAV design provides improved maneuverability and agility, making it particularly useful in applications where traditional aircraft may not be effective.

In conclusion, this report demonstrates the feasibility of a flapping wing aerial vehicle as a potential alternative to traditional aircraft for specific applications. The FWAV prototype's stable flight performance validated the design's effectiveness, offering valuable insights into the design and implementation of a flapping wing aerial vehicle.

ACKNOWLEDGEMENTS

We begin in the name of Allah, the Creator of the universe, and seek His blessings upon the Prophet Muhammad (PBUH) and his family and companions. We are grateful to Allah for granting us the strength and patience to overcome any challenges we faced during this project.

We extend our gratitude to our supervisor, Dr. Emad Uddin for his invaluable assistance and guidance. Their constructive feedback and suggestions were instrumental in the project's success. His timely contributions were essential in shaping the project into its final form, and we express our sincerest appreciation for his support.

We are honored to have had the opportunity to work on the “Flapping Wing Aerial Vehicle” project under the supervision of Dr. Javaid Iqbal, our principal. We also thank our fellow students who provided us with invaluable assistance during our research. Throughout the process, we discovered new and interesting connections between various engineering fields, expanding our knowledge.

ORIGINALITY REPORT

We certify that this research work titled “Flapping Wing Aerial Vehicle” is our own work. The work has not been presented elsewhere for assessment. The material that has been used from other sources has been properly acknowledged / referred and following is the originality report from Turnitin.

Signature of Students



Feroze Sharjeel

290744



Toheed Ahmad

283594



Ans Sadiq

294916



Ahad Ali Meer

298050

Thesis

ORIGINALITY REPORT

9%

SIMILARITY INDEX

6%

INTERNET SOURCES

2%

PUBLICATIONS

3%

STUDENT PAPERS

PRIMARY SOURCES

1

ebin.pub

Internet Source

3%

2

Submitted to Higher Education Commission
Pakistan

Student Paper

1%

3

www.ijser.org

Internet Source

1%

4

Submitted to University of Witwatersrand

Student Paper

1%

5

Salman A. Ansari, Kevin Knowles, Rafał
Żbikowski. "Design Guidelines for Flapping-
Wing Micro UAVs", SAE International, 2005

Publication

<1%

6

Mohammad H. Sadraey. "Aircraft Design",
Wiley, 2012

Publication

<1%

7

kupdf.net

Internet Source

<1%

8

Salman A. Ansari, Kevin Knowles, Rafał
Zbikowski. "Insectlike Flapping Wings in the

<1%

Hover Part II: Effect of Wing Geometry", Journal of Aircraft, 2008

Publication

9	Submitted to University of Warwick Student Paper	<1 %
10	research-information.bris.ac.uk Internet Source	<1 %
11	ieeexplore.ieee.org Internet Source	<1 %
12	Submitted to University of Illinois at Urbana-Champaign Student Paper	<1 %
13	fics.nust.edu.pk Internet Source	<1 %
14	Submitted to University of Nottingham Student Paper	<1 %
15	Submitted to Coventry University Student Paper	<1 %
16	dspace.lboro.ac.uk Internet Source	<1 %
17	Submitted to Kingston University Student Paper	<1 %
18	Submitted to Virginia Commonwealth University Student Paper	<1 %

19	M. Asjid Tanveer, M. Jawad Khan, M. Jahangir Qureshi, Noman Naseer, Keum-Shik Hong. "Enhanced Drowsiness Detection Using Deep Learning: An fNIRS Study", IEEE Access, 2019 Publication	<1 %
20	www.researchgate.net Internet Source	<1 %
21	Izhar Ullah, Lesley M. Wright, Chao-Cheng Shiau, Je-Chin Han, Zhihong Gao, Andrea Stanton. "Film Cooling Comparison of Full-Scale Turbine Vanes Using the Pressure Sensitive Paint Technique", Journal of Turbomachinery, 2023 Publication	<1 %
22	Submitted to University of Central Lancashire Student Paper	<1 %
23	jaxa.repo.nii.ac.jp Internet Source	<1 %
24	Sadaqat Ali, Ahmad Majdi Abdul Rani, Zeeshan Baig, Syed Waqar Ahmed et al. "Biocompatibility and corrosion resistance of metallic biomaterials", Corrosion Reviews, 2020 Publication	<1 %

TABLE OF CONTENTS

ABSTRACT	2
ACKNOWLEDGEMENTS	3
ORIGINALITY REPORT	4
TABLE OF CONTENTS	8
LIST OF FIGURES & TABLES	11
CHAPTER 1	13
CHAPTER 2	15
2.1 <i>WINGS</i> :.....	15
2.2 <i>MECHANISM</i> :	19
2.3 <i>ELECTRONICS</i> :.....	22
2.3.1 <i>FLIGHT CONTROLLER</i> :.....	22
2.3.2 <i>MOTORS</i> :	23
2.3.3 <i>BATTERY</i> :.....	23
2.3.4 <i>TAIL</i> :.....	24
2.3.5 <i>FUSELAGE DESIGN</i> :.....	25
CHAPTER 3	26
3.1 <i>MECHANISM SELECTION</i> :	28
3.2 <i>TOTAL WEIGHT, SPAN, AND FLAPPING FREQUENCY</i> :	28
3.3 <i>ELECTRONICS</i> :.....	29
3.3.1 <i>MOTOR</i> :.....	30
3.3.2 <i>ELECTRONIC SPEED CONTROLLER</i> :	30
3.3.3 <i>BATTERY</i> :.....	31
3.3.4 <i>RADIO SYSTEMS</i> :	32
3.3.5 <i>FLIGHT CONTROLLER/STABILIZER</i> :.....	32

3.4 MECHANISM DESIGN:.....	33
3.4.1 GEAR TRAIN.....	33
3.4.2 FOUR BAR LINKAGE DESIGN.....	34
3.5 TAIL:.....	35
3.5.1 C-TAIL DESIGN:.....	35
3.5.2 V-TAIL:.....	37
3.6 WING DESIGN:.....	37
3.6.1 WING CONFIGURATION:.....	38
3.6.2 WING SKELETON:.....	39
3.6.3 WING SKELETON MATERIAL:.....	40
3.6.4 WING MEMBRANE MATERIAL:.....	40
3.7 FUSELAGE:.....	40
3.7.1 SKELETON:.....	40
3.7.2 BODY:.....	41
3.8 SIMULATIONS.....	41
3.8.1 FEA ANALYSIS OF GEAR TRAIN:.....	41
3.8.2 FEA ANALYSIS OF MECHANISM:.....	42
3.8.3 CFD ANALYSIS ON WINGS:.....	43
3.9 FINAL TESTING:.....	44
3.9.1 RUDDER AND ELEVATOR:.....	44
3.9.2 STABILITY TESTING:.....	44
3.9.3 THRUST TESTING:.....	45
CHAPTER 4.....	46
4.1 FINAL PARAMETERS:.....	46
4.2 EQUIPMENT SELECTION:.....	47
4.2.1 MOTOR:.....	47
4.2.2 SERVO MOTOR:.....	48
4.2.3 BATTERY:.....	48

4.2.4 FUSELAGE MATERIAL:.....	49
4.2.5 MECHANISM:	49
4.2.6 WINGS:.....	50
4.2.7 TAIL:.....	50
4.3 FEA ANALYSIS:.....	51
4.3.1 STRUCTURAL ANALYSIS OF GEAR TRAIN.....	51
4.3.2 TRANSIENT ANALYSIS OF OUTBOARD WING HINGE MECHANISM:	53
4.4 CFD ANALYSIS:	55
4.5 MANUFACTURING PLAN:.....	56
4.5.1 PROCUREMENT:	56
4.5.2 3D PRINTING:	56
4.5.3 ASSEMBLY:.....	56
4.5.4 EQUIPMENT TESTING:.....	57
4.5.5 IMPROVEMENTS:	57
4.6 TESTING RESULTS:.....	57
4.6.1 RUDDER AND ELEVATOR:	57
4.6.2 STABILITY TESTING:	57
4.6.3 THRUST TESTING:.....	58
CHAPTER 5	59
REFERENCES.....	60
ANNEXURE A	62

LIST OF FIGURES & TABLES

FIGURE 2.1: LEADING EDGE TAPE AND DESIGN PARAMETER _____	17
FIGURE 2.2: ESTIMATED MASS OF THE WINGS _____	18
FIGURE 2.3: WING MEMBRANE MATERIALS _____	19
FIGURE 2.4: TYPES OF FLAPPING MECHANISMS _____	20
FIGURE 2.5: FLAPPING MECHANISM DESIGN PROTOTYPES USED BY LUNG-JIEH YANG AND BALASUBRAMANIAN ESAKKI [4] _____	21
FIGURE 3.1: FLOWCHART FOR DESIGN METHODOLOGY _____	27
TABLE 3.1: TAIL COEFFICIENTS _____	36
FIGURE 3.1: WING CONFIGURATION FOR 20CM SPAN _____	38
FIGURE 3.2: WING CONFIGURATION FOR 80CM SPAN _____	39
FIGURE 3.3: WING SKELETON FOR 80CM SPAN _____	39
FIGURE 3.4: WING MESH _____	43
FIGURE 3.5: FINAL MODEL FOR STATIC TESTING _____	45
TABLE 4.1: FINAL PARAMETERS _____	46
FIGURE 4.1: RENDERED FINAL MODEL _____	47
FIGURE 4.2: A2212 1000KV BRUSHLESS DC MOTOR _____	48
FIGURE 4.3: TOWERPRO SG90 PLASTIC GEAR SERVO _____	48
FIGURE 4.4: 4MM CARBON FIBER _____	49
FIGURE 4.5: GEAR MECHANISM _____	50
FIGURE 4.6: WING CONFIGURATION WITH ORCON PAPER _____	50
FIGURE 4.7: TAIL CONFIGURATION WITH FOAM BOARD _____	51
FIGURE 4.8: VON-MISES STRESS FOR GEAR ASSEMBLY _____	52
FIGURE 4.9: ZOOMED VERSION OF VON-MISES STRESS _____	52
FIGURE 4.10: FACTOR OF SAFETY ANALYSIS FOR GEAR ASSEMBLY _____	53
FIGURE 4.11: EQUIVALENT STRESS ANALYSIS FOR OUTBOARD WING HINGE _____	53

FIGURE 4.12: TOTAL DEFORMATION ANALYSIS FOR OUTBOARD WING HINGE _____	54
FIGURE 4.13: EQUIVALENT ELASTIC STRAIN FOR OUTBOARD WING HINGE _____	54
FIGURE 4.14: PRESSURE DISTRIBUTION ON WING MEMBRANE _____	55

CHAPTER 1

INTRODUCTION

The concept of emulating bird flight has long captivated the imagination of human inventors. The effortless ease and graceful agility with which natural fliers take to the air vastly surpasses the state-of-the-art in modern aircraft and their control systems. While fixed-wing aircraft and rotorcraft have their strengths, such as efficient thrust production and lift generation, they are unable to match the maneuverability and versatility of their avian counterparts.

Flapping Wing Aerial Vehicles (FWAVs), on the other hand, attempt to replicate the complex flapping motion of birds and insects in order to generate lift and maneuverability. The design of these vehicles entails careful consideration of factors such as wing shape, size, and kinematics, as well as power source and control system. Despite the challenges associated with FWAV design and control, recent advances in materials, electronics, and control systems have made FWAVs increasingly viable.

In addition to their superior agility and maneuverability, FWAVs have the potential to be more efficient than traditional aircraft as they can generate lift without the need for forward velocity. This makes them ideal for a wide range of applications, such as surveillance, search and rescue, and environmental monitoring.

This research project aims to investigate the design, control, and performance of a FWAV. Specifically, the project will focus on developing a prototype FWAV, analyzing the aerodynamics of flapping wings, designing and fabricating the FWAV prototype,

developing a control system for the FWAV, and evaluating its performance in various flight regimes.

Overall, the development of FWAVs has the potential to revolutionize the field of aerial robotics and enable new applications in fields such as agriculture, environmental monitoring, and disaster response.

CHAPTER 2

LITERATURE REVIEW

The focus of this literature review was based totally on our problem statement. Our problem statement is “The development of flapping wing aerial vehicle capable of flying efficiently while carrying the electronics necessary for its control.” So, based on that problem statement, we have studied the aerodynamics and flight of ornithopters, wing configurations and skeleton design, different types of flapping mechanisms and their designs, fuselage design, tail design and its types, material selection, and the electronics related to ornithopter stable flight and control.

A basic review of all research papers and books which were studied to complete the project deliverables are as follows:

2.1 Wings:

Nathan Chronister [\[1\]](#) has stated about the aerodynamics of flapping wings by discussing some basic terminologies like angle of attack, lift, drag, stall, advance ratio, coefficient of lift, pitch, and vortex theory of lift. Moreover, he has also discussed about lift from membrane wings and spanwise variation in lift and thrust forces of flapping wings. According to him, the central portion of wing is mainly responsible for lift while tip of wing is responsible for both lift and thrust because of its twisting during upstroke and downstroke.

Lung-Jieh Yang and Suseendar Marimuthu [2] have discussed about the effect of wingspan on ornithopter mass and flapping frequency. According to them, a 20cm span flapping wing aerial vehicle (FWAV) should have the mass of about 11 g and its flapping frequency should be 15 Hz. These figures are calculated from equation (1) and (2)

$$b = 1.17m^{0.39}; (birds) \quad (1)$$

$$fw = (3.98)m^{(-0.27)}; (birds) \quad (2)$$

Kushal Jadhav and Harshada Javheri [3] have studied the material properties wing skeleton. According to their research paper, it is important to choose a material with high rigidity, long durability, low weight, strong chemical resistance, heat tolerance, and low thermal expansion. Over steel and aluminum, carbon fiber was selected as the material for the wing frame to meet all these requirements.

Lung-Jieh Yang and Balasubramanian Esakki [4] have performed experiments in wind tunnel for different configurations (S1 – S6) of flapping wings with 20-degree inclined angle at different speeds. In these configurations, leading edge tape width is changed accordingly as shown in figure. The important observations of these experiments are:

1- The tape's width can be chosen between 0.5 cm (S2) and 1.0 cm if the lifting phenomenon is required (S3).

2- The wing membrane is strengthened by adjusting the leading-edge tape width from 0.5 to 1.5 cm if the thrust production is more of a concern (S5).

Leading-Edge Tape and Design Parameter for PE Wings of 17 μm Thick

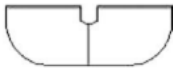


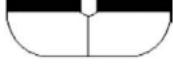
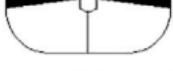
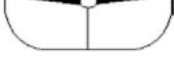
ID	Tape Width	Tape Shape	Wing Mass (gram)
S1	0		0.226
S2	0.5 cm		0.297
S3	1.0 cm		0.330
S4	1.5 cm		0.376
S5	0.5-1.5 cm		0.335
S6	1.5-0.5 cm		0.335

Figure 2.1: Leading Edge Tape and Design Parameter

Similarly, they also performed some experiments with various diameters of carbon fiber rods and their angle of positioning with respect to leading edge (S7 – S11) as shown in figure. The observation from these experiments is:

- 1- The lift force greatly increases along with the frequency of flapping.
- 2- The S8 wing rib is heavier and thicker than the S7 wing rib, which reduces the frequency of flapping and, consequently, the lift force.
- 3- The lift force is reduced because the S9 wing rib is closer to the leading edge and there is more wing area between it and the trailing edge. The larger wing membrane is incapable of supporting itself.
- 4- The S10 wing rib has the highest flapping frequency because it is situated closer to the trailing edge.

Carbon Fiber Ribs and an Estimated Mass of the Wings





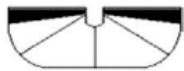
ID	Tape Width	Carbon Fiber Diameter and Angle	Wing Configure	Weight (gram)
S7	0.7 cm	$\phi 0.3$ mm, 30°		0.360
S8	0.7 cm	$\phi 0.5$ mm, 30°		0.392
S9	0.7 cm	$\phi 0.3$ mm, 20°		0.364
S10	0.7 cm	$\phi 0.3$ mm, 40°		0.366
S11	0.5-1.5 cm	$\phi 0.3$ mm, 30°		0.394

Figure 2.2: Estimated Mass of the Wings

Compared to other wings (S7-S10), the S11 wing produced the most lift force. The net thrust force for S7-S11 wing designs is calculated in a similar manner. The findings are:

1- S11 has achieved a maximum net thrust of 4.01 gf in zero wind speed conditions, giving it the highest takeoff acceleration.

2- It appears that the S11 uses little power to produce a lot of net thrust.

So, S11 configuration can be selected as the final configuration for wing design.

Sutthiphong Srigraromn and Woei-Leong Chan [5] performed experiments in wind tunnel on three different wing designs to observe lift and thrust generation characteristics. According to the results, the thrust generation for Orcon flat wing has better results as compared to others.

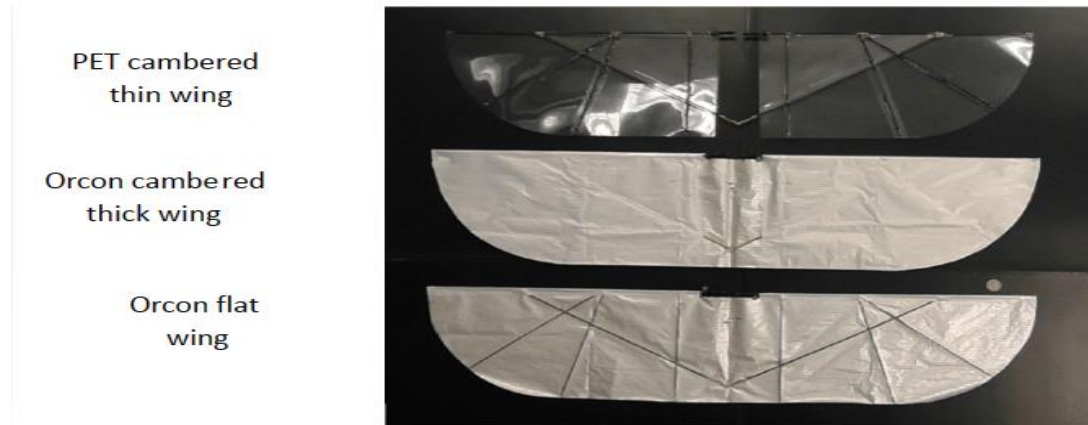


Figure 2.3: Wing Membrane Materials

Salman A. Ansari, Kevin Knowles and Rafał Żbikowski [6] have discussed about the effect of various wing parameters like aspect ratio, wing area and wingspan on the performance of flapping wings. In their study, lift and thrust forces increases with an increase in wing length and aspect ratio but the lift to torque ratio decreases because of the vortex breakdown that ensues in the outboard regions as the wing gets longer. Moreover, the increase in wing area cause and increase in lift force but the lift to torque ratio increases up to a certain point then decreases or remains almost constant. This is because the torque would be increasing at the same rate so does the power requirement.

2.2 Mechanism:

Nathan Chronister [1] has stated about different types of flapping mechanisms. The designs he has discussed are:

- 1- Staggered Crank (It converts rotary motion into reciprocating motion using two cranks that are arranged in a staggered position).

- 2- Outboard Wing Hinge (In this mechanism, a hinge is in the outer part of wing to allow for movement of flap).

3- Dual Crank (It converts rotary motion into reciprocating motion using two parallel cranks).

4- Transverse Shaft (In this mechanism, a transverse shaft is positioned perpendicular to the direction of motion, transmitting power and torque between two components that are parallel to each other)

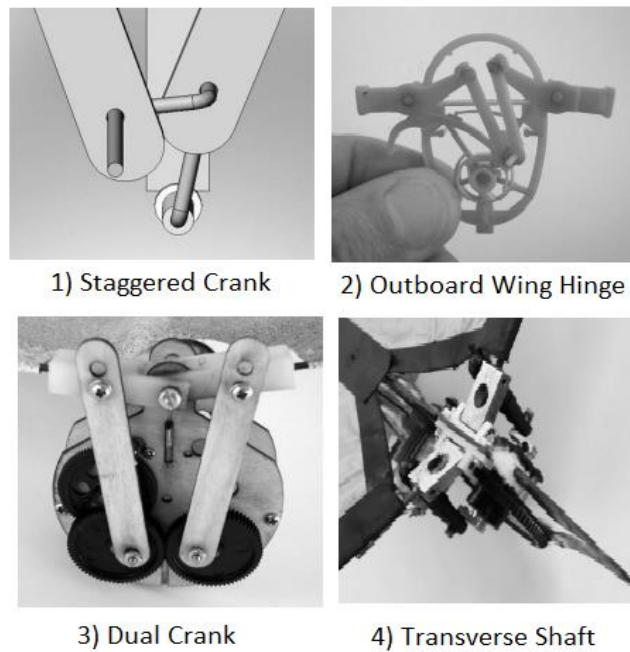


Figure 2.4: Types of Flapping Mechanisms

Lung-Jieh Yang and Balasubramanian Esakki [4] have tested three different design prototypes of flapping mechanisms. These three are FBL Mechanism, Stephenson's Mechanism and Evans Mechanism as shown in figure 2.7.

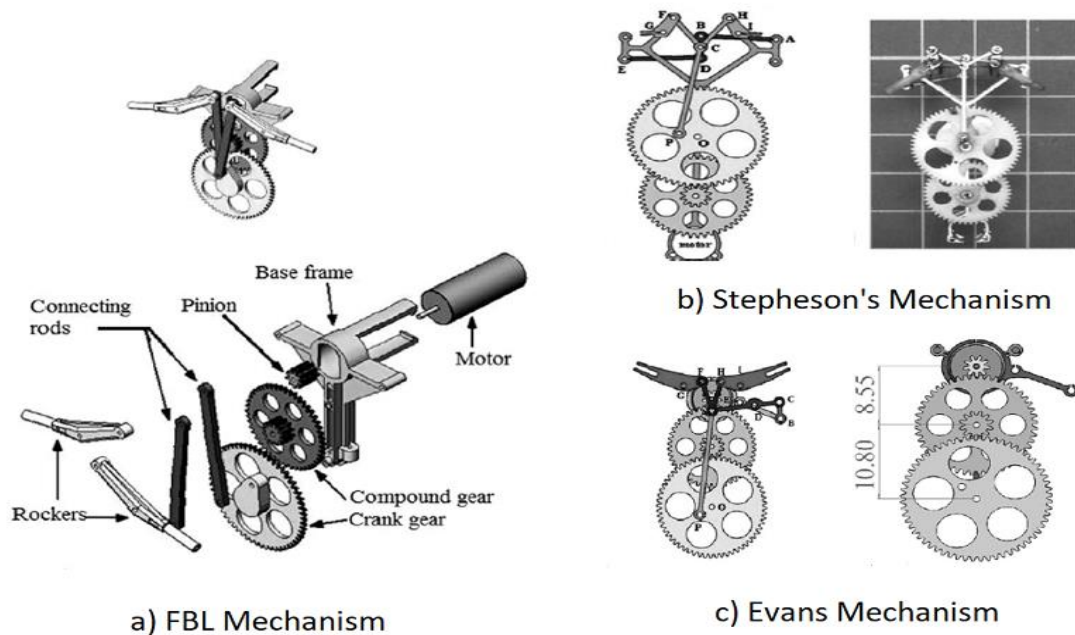


Figure 2.5: Flapping mechanism design prototypes used by Lung-Jieh Yang and Balasubramanian Esakki [4]

The summary of their experimentation on these design prototypes is as follows:

1. The wind tunnel testing and real flight testing of Golden-Snitch using the FBL mechanism were demonstrated. A cruising condition of zero net thrust force was found at the inclined angle of 40° , driving voltage of 3.7 V (with the flapping frequency of 14 Hz), and maximum lift force of 9.8 gf. However, the phase lag between two wings was 3.2° , which induces a non-synchronized lift difference between two wings that may cause the FWMAV to spiral down.
2. The Stephenson mechanism and Evans mechanism effectively increased the flapping stroke angle and the lift and minimized the phase lag close to zero simultaneously. It was found that the aerodynamic performance of the Evans mechanism was better than the Stephenson mechanism. Evans mechanism attained

a maximum flapping stroke angle of 80° , and the motor-mechanism configuration was very similar to the FBL mechanism.

Joshua Adcock of OrnithopterX [\[7\]](#) has developed an Excel spreadsheet, named as “Ornithopter Crank Designer”, to calculate the dimensions for ornithopter’s crank mechanisms. It can calculate the optimal dimensions for symmetrical flapping by providing some design parameters such as range of flapping motion.

Lung-Jieh Yang and Balasubramanian Esakki [\[4\]](#) studied and experimented various manufacturing methods such as EDWC, PIM and 3D Printing to manufacture flapping mechanism parts of FWAV. They have discussed about assembly of mechanism parts, estimation of flapping frequency, flapping angle, total mass of flapping mechanism and endurance of mechanism parts. Moreover, they performed the aerodynamic analysis of FWAV using custom test rig apparatus to compare three manufacturing methods and different 3d printed materials. The 3d printed was able to provide efficient flapping frequency and lift.

2.3 Electronics:

2.3.1 Flight Controller:

According to a study by [K. Adarsh et al. \(2020\) \[8\]](#), the most important factors to consider when selecting a flight controller for an RC plane are the number of channels, the maximum input voltage, the operating frequency, and the type of sensors used. The number of channels refers to the number of input/output ports that the flight controller can handle. A higher number of channels allow for more advanced functions, such as autopilot and GPS navigation. The maximum input voltage is crucial because it determines the maximum

power that the flight controller can handle. The operating frequency is also important since a higher frequency allows for faster data processing and more accurate stabilization. Finally, the type of sensors used by the flight controller, such as gyroscopes and accelerometers, affects the accuracy and responsiveness of the aircraft.

2.3.2 Motors:

According to a study by M. K. Ali et al. (2020) [9], the most important factors to consider when selecting a brushless motor for UAVs are the motor's size and weight, maximum thrust, maximum efficiency, and maximum power output. The size and weight of the motor are crucial because they affect the overall weight and size of the UAV. A smaller and lighter motor can improve the UAV's agility and maneuverability, but it may also reduce the maximum thrust and efficiency. Therefore, a balance must be struck between size, weight, and performance.

The maximum thrust of the motor determines how much weight the UAV can lift and how fast it can accelerate. It is essential to choose a motor that can provide enough thrust for the UAV's weight and desired flight characteristics. The maximum efficiency of the motor affects the UAV's endurance and range. A more efficient motor can prolong the UAV's flight time and reduce the need for frequent battery changes.

2.3.3 Battery:

According to a study by J. G. Simpson et al. (2020) [10], the most important factors to consider when selecting a battery for UAVs are the battery's energy density, capacity, discharge rate, weight, and size. The energy density of the battery refers to the amount of energy it can store per unit of weight or volume. A higher energy density can increase the UAV's flight time and range, but it may also increase the battery's cost and safety risks.

The battery's capacity is another crucial factor that determines how much energy it can provide to the UAV's motors and electronics. A higher capacity can prolong the UAV's flight time, but it may also increase the battery's weight and size. The discharge rate of the battery affects how quickly it can deliver energy to the UAV's systems, which is essential for high-speed maneuvers and emergencies.

2.3.4 Tail:

The V-tail is a type of aircraft tail configuration that utilizes two surfaces arranged in a V-shape to perform the functions of both a horizontal stabilizer and vertical fin. The design of a V-tail involves numerous considerations, including aerodynamic performance, structural integrity, and manufacturability. In this literature review, we will examine a paper by Daniel Raymer [\[11\]](#) which provides a comprehensive overview of the design process for V-tails.

Raymer's paper begins by outlining the benefits and drawbacks of using a V-tail configuration. One of the main advantages is that the V-tail can provide better aerodynamic efficiency compared to a conventional tail configuration, which can lead to increased range and fuel economy. Additionally, the V-tail can improve aircraft performance in certain flight regimes, such as during high angle-of-attack maneuvers. However, there are also several challenges associated with designing a V-tail, such as structural complexity, control system design, and stability and control characteristics.

2.3.5 Fuselage Design:

The paper "Fuselage Aerodynamics and Weight Trade-Off at Low-Speed Ornithopter Flight" [\[12\]](#) published in the IEEE (Institute of Electrical and Electronics Engineers) Transactions on Aerospace and Electronic Systems journal, discusses the trade-offs between fuselage aerodynamics and weight for low-speed ornithopter flight.

The paper begins by introducing the concept of ornithopters, which are aircraft that fly by flapping their wings like birds. Ornithopters have unique flight characteristics and challenges compared to fixed-wing aircraft, including complex wing kinematics and significant variations in aerodynamic forces during flapping motion. The authors then explain that the fuselage of an ornithopter plays a critical role in aerodynamic performance, stability, and weight distribution.

The paper then discusses the trade-offs between aerodynamic performance and weight for ornithopter fuselage design. The authors argue that the weight of the fuselage is critical for achieving efficient flight, as a heavy fuselage can increase the energy required for flapping motion and reduce overall flight endurance. The authors analyze the impact of different fuselage materials, such as foam, carbon fiber, and balsa wood, on the weight and structural integrity of the ornithopter.

CHAPTER 3

METHADODOLOGY

From the extensive literature review, it was clear that the controlling factor in the design of a flapping wing aerial vehicle is its total weight. The biggest contributor to the weight of the vehicle proved to be the on-board electronics. To make an initial estimate about the weight, we began by choosing a design that was ideal for relatively small span ornithopters and engendered minimal phase difference in the wing flaps, which was found to be Outboard Wing Hinge Mechanism. The choice of design had direct effect on the type of electronics that were to be incorporated; for instance, if we had preferred a single crank configuration over a dual crank configuration, we would have needed a motor of different torque and changing the motor meant changing all the other electronics.

Once the mechanism was defined, we searched the literature for similar designs and made a rough choice of electronics, incrementing each value by a few grams as a safety net. An initial estimate of the weight was made, and the span was determined. From here on forward the span took the governing role and controlled most of the design choices. The following flowchart aims to give an overview of the design methodology:

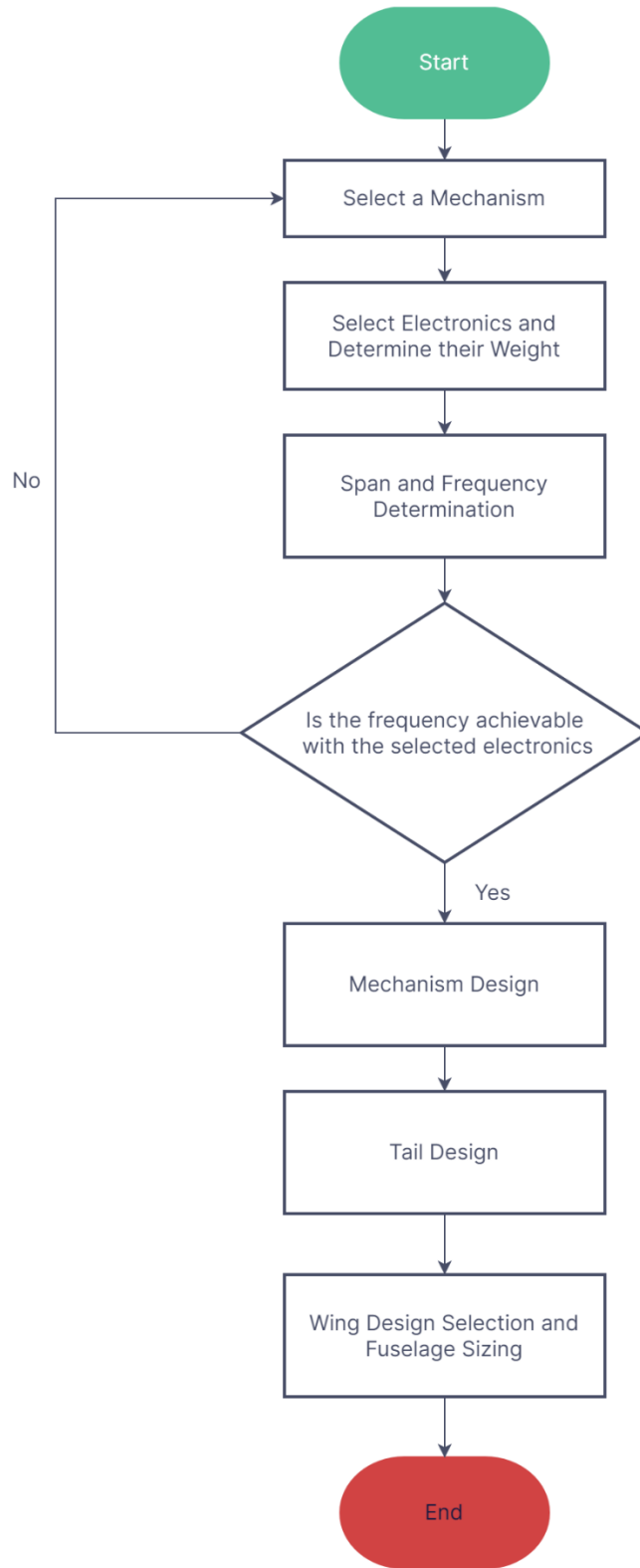


Figure 3.1: Flowchart for Design Methodology

3.1 Mechanism Selection:

The literature review provided us with four intuitive mechanisms. Each mechanism had its own features and required different fabrication techniques. Having gone through the pros and cons of all the mechanisms, we decided on moving forward with Outboard Wing Hinge design for the following reasons:

- Ubiquitous in Ornithopters of span between 20cm to 60cm.
- Low phase difference between the two wings.
- Less moving parts and stable configuration.
- Ample documentation.

3.2 Total Weight, Span, and Flapping Frequency:

Before, in the literature review section of this document, it was discussed in detail that the span and flapping frequency of a flapping wing aerial vehicle are directly dependent on its weight. The equations obtained from the literature allowed the expression of any two quantities—of the three aforementioned quantities—in terms of any one quantity. Since a crude estimate of the weight could be made early on, it was chosen as the controlling factor.

Making these fundamental choices at the beginning is crucial to many of the other design choices that must be made in the future. Owing to the use of the project for surveillance purposes, it was paramount that the span of the aircraft should be kept as small as possible. Large span birds make more noise and are easier to detect from a distance. Keeping the span small is equivalent to a smaller payload, which is controlled by the mass of the electronics. This led to a thorough research of the market to search for light-weight electronics that performed adequately in controlling the flight of an ornithopter. Adding a

few grams to introduce a safety net and a few more to account for the weight of the fuselage, a value for the mass of the ornithopter was obtained.

Using the following relations, the span and flapping frequency can be obtained:

$$\textit{Span} = 1.17 \textit{mass}^{0.39}$$

$$\textit{Flapping Frequency} = 3.98 \textit{mass}^{-0.27}$$

With the span and flapping frequency, the more important aspects of the design can be started.

3.3 Electronics:

The outboard wing hinge design relies on a simple compound gear train to transfer the torque and angular speed of the motor to the crank of a four-bar linkage. Since both rockers were driven from the same crank, we only needed one motor to control the whole mechanism. The choice of motor controlled our choice of ESC and battery.

The rear end of the ornithopter comprises of control surfaces—rudder and elevator or in our case two rudder-vators—which need one servo per control surface. Once the choice of motor and servos is sorted, one can comfortably move onto picking a RC radio, video transmission system, and flight controller—the last two being optional additions.

The following headings will comprehensively explain the underlying methodology for the choice of electronics stated in results and discussion portion of this document.

3.3.1 Motor:

After evaluating several factors, including efficiency, availability, operating temperatures, and speed, the decision was made to select a brushless motor for the motor selection process.

With the required frequency of wing flaps and weight limit, a few motors were shortlisted. The exact constraints that were put at this stage were as follows: the Kv rating of the motor should be above a set value—the set value was determined using the required frequency at the rocker and the gear ratios available using procured gears—and torque of the motor should be comparable to the motors used in similar designs.

To determine a baseline value for Kv of the motor, the following relations were used:

$$Gear\ Ratio = \frac{\omega_{motor}}{\omega_{crank}}$$

$$\omega_{motor} = \omega_{crank} \times Gear\ Ratio$$

$$Kv_{baseline} = \frac{\omega_{motor}}{Volts\ from\ Battery}$$

The number of cells a motor can operate on is usually mentioned on its specifications sheet. Multiply the number of cells with 3.7V to get the maximum operating voltage.

3.3.2 Electronic Speed Controller:

An electronic speed controller is crucial for the operation of a brushless motor. It hosts the battery eliminator circuit which performs the job of supplying appropriate volts to the brushless motor and, as the name suggests, is also responsible for the control of the motor speed. ESCs connect directly to the motor and battery, with two extra wires for the receiver.

The choice of ESC depends on the maximum continuous current being drawn by the brushless motor. A rule of thumb is to keep the current rating of the ESC 10A above the maximum current being drawn by the motor. Choosing an ESC with a rating comparable to the motor will cause the ESC to heat up quickly and even catch on fire.

3.3.3 Battery:

A wide variety of batteries, widely differing in size and capacity, can be found on the market that can function adequately in RC vehicles. Though batteries can be classified in a number of ways but the classification of interest here is the material they use to store charge. The decision to move forward with lithium polymer batteries is based on several reasons, the most important of which are: have lighter weight for the same capacity, possess greater charge capacity, safe packaging, and market availability.

A typical lithium polymer battery specification sheet will include the following information: Number of cells, mAh rating, discharge, and its weight.

A few considerations should be made before choosing a battery. Firstly, the number of cells in the battery should match the number of cells the motor operates on; or at-least lie in range. Secondly, to determine the mAh rating, refer to the following procedure:

$$\text{Amp} - \text{Hours} = \text{Maximum Continuous Current Drawn by Motor} \times \text{Operation Time in Hours}$$

For instance, if a motor—that draws 2.8 amperes of continuous current—needs to be run for 10 minutes, the amp-hour rating for a battery that could achieve that is given by:

$$\text{Amp} - \text{Hours} = 2.8 \times \frac{10}{60}$$

$$\text{Amp} - \text{Hours} = 0.416$$

$$mAh = 416$$

So, any battery with mAh rating greater than 416 is appropriate for the case defined above.

Lastly, the discharge rate is selected by multiplying the C rating with the mAh value and keeping it over 130 percent of the maximum power system discharge. This step concludes the battery selection process.

3.3.4 Radio Systems:

The radio system choice for the model depended a lot on what was present on campus. The reason for this being the exorbitantly high prices associated with the transmitter/receiver combo. Other considerations like the mode, configuration, and frequency of communication were not paid much attention to as they are irrelevant, or the adjoining receiver already takes care of that.

Since receiver is a lightweight component and does not need any complementary electronics, only one constraint is put on the choice of radio system: that it has at-least 3 channels for communication; one for the brushless motor and the rest for the servo motors.

3.3.5 Flight Controller/Stabilizer:

The use of a flight controller/stabilizer provides the much-needed stability for the smooth flight of ornithopters. It autocorrects for any discrepancies created in the straight flight of the robotic bird and brings it to an orientation that puts it back on the original path.

At this stage, one can go two ways. Either take an Arduino nano and program it to function as a flight controller/stabilizer or save themselves of the extra work and pick a flight controller/stabilizer. This provides us more time to work on the mechanical design of the

mechanism used for power transmission and not hamper the progress by writing ingenious code for incorporating functions of a flight controller/stabilizer.

The flight controller choice was dependent on many parameters in addition to the weight restriction. For starters, it should at-least have 3 PWM ports and 2 UARTS channels. Furthermore, it should be compatible with the opensource Betaflight software. Lastly, its maximum continuous current rating should be well below what the battery can provide, and its operating voltage should be the same as that of your battery or a BEC must be paired with it.

3.4 Mechanism Design:

Stripping Outboard Wing Hinge Mechanism to its core, it contains a simple compound gear train and a crank rocker four-bar linkage, whose crank is attached to the output gear of the train. Naturally, the design of the two is related as the distance between one of the shoulders and crank axis acts as the ground link of the four-bar mechanism. Keeping that in mind, it was obvious that the design process will start with the gear train and conclude on the four-bar linkage.

3.4.1 Gear Train

The output flapping frequency of the ornithopter was determined analytically with respect to the weight and wingspan, given the input torque and frequency of the motor gear train was to be selected to reduce the speed and increase the torque according to design.

$$\frac{w_1}{w_4} = \text{Gear ratio}$$

$$w_1 = \text{RPM of motor}$$

$$w_4 = \text{Required flapping frequency}$$

First, gears were procured and sorted according to module number and then appropriate module number was selected to give optimum strength.

FEA analysis was done on the gears using SolidWorks to ensure the strength of the gears and calculate the factor of safety according to applied torque by the motor. Then desired combination of gears was selected to provide the speed reduction analogous to design requirements within size and strength constraints.

3.4.2 Four Bar Linkage Design

The linkage design relies a lot on assumption and standards. Linkage design starts with selecting the wing sweep angle and average dihedral. Positive dihedral provides lateral stability, so ornithopters require slightly positive average dihedral. Flapping amplitude can vary from 45 and 60 degrees. Determine the amount of horizontal space between wing hinges; keep it at-least one-tenth of the wingspan and enough to accommodate the lever radius, the height of the wing hinges above the crank axle; determined by the procured gears, and the wing lever radius; the wing lever radius should be at least one-tenth of one of the wing spars lengths but setting a greater value is encouraged. The clearance between wing levers should be fairly small, and the offset angle between the wing spar and wing lever should be about 20 degrees. To determine the correct length for connecting rods, measure the distance from the crank center to the fully raised wing lever and to the lowered wing lever. The connecting rod length is half the sum of crank center to fully raised wing and crank center to a completely lowered wing distance. Finally, determine the appropriate crank radius by halving the difference between the aforementioned quantities and draw the circular path of the crank arm.

3.5 Tail:

Due to the absence of ailerons or any mechanism to control the angle of attack of the wings, the tail of bird hosts all the control surfaces, namely rudder and elevator. The elimination of the third control surface—that would have introduced the weight of two more servos and a servo controller—was crucial to keep the span small. Moreover, to increase the resemblance of the robot with an actual bird, a v-tail is preferred over c-tail. The process of designing any tail other than the c-tail is to first get all the dimensions for the c tail and then move onto the required design.

3.5.1 C-tail Design:

For the design of the tail, the tail volume coefficient method is used. Tail volume coefficients relate the span and area of the wing with the surface area of the tail. Knowing the span, area, length between the aerodynamic centers of the wing and tail, and mean chord length of the wing, the tail volume coefficient method gives the area of the horizontal and vertical tail.

$$c_{ht} = \frac{L_{ht}S_{ht}}{S_w\bar{C}_w}$$

$$c_{vt} = \frac{L_{vt}S_{vt}}{S_w b_w}$$

Here,

c_{ht} is the horizontal tail volume coefficient.

c_{vt} is the vertical tail volume coefficient.

L_{ht} is the distance between the aerodynamic center of the wing and the horizontal tail.

L_{vt} is the distance between the aerodynamic center of the wing and the vertical tail.

S_w is the area of the wing.

S_{ht} is the area of the horizontal stabilizer.

S_{vt} is the area of the vertical stabilizer.

b_w is the span of the wing.

$\overline{C_w}$ is the length of the mean aerodynamic chord.

For the coefficients the following table can be referred:

Table 3.1: Tail Coefficients

	Horizontal c_{ht}	Vertical c_{vt}
Sailplane	0.5	0.02
Homebuilt	0.5	0.04
Jet Fighter	0.4	0.07
Jet Trainer	0.7	0.06

For our case, we used a horizontal tail coefficient of 0.4 and a vertical tail coefficient of 0.04. It should be noted that the table mentions values for actual planes and the chosen coefficients should be slightly reduced for RC planes. Moving over to the other unknown variables: the distance between the aerodynamic centers is to be assumed at this stage and for low-speed RC planes a value of 60 percent of the total is deemed adequate.

The area of rudder is chosen to be 50 percent of the total vertical stabilizer area and area of the elevator is kept 40 percent of the total horizontal stabilizer area.

3.5.2 V-tail:

Having obtained all the dimensions of a conventional tail, the following relations can be used to make a jump between the two:

$$S_{V-Tail} = S_{ht} + S_{vt}$$

$$Dihedral\ Angle = \arctan\left(\sqrt{\frac{S_{vt}}{S_{ht}}}\right)$$

Here S_{V-Tail} is area of both halves of the v-tail. Using both these parameters a V-tail can be sketched out with the following taper and aspect ratio:

3.6 Wing Design:

The design of a completely new wing was deemed impractical because the experimentation demands wing tunnel and load cell, and the CFD analysis of flapping wings requires high computational cost and time. So, it was decided to choose researched proved wing design and adjust that design according to our wingspan. Before going into detail, it is important to know about the term “Aspect Ratio.”

$$Aspect\ Ratio = \frac{S^2}{A}$$

Where ‘S’ is wingspan and ‘A’ is wing area.

3.6.1 Wing Configuration:

Upon reviewing many research papers, the wing configuration which was selected is of 20cm span with aspect ratio of 3.51. It is the wing configuration on which Lung-Jieh Yang and Balasubramanian Esakki [4] has performed wing tunnel experiments for lift and thrust calculations. This wing configuration is shown in the following figure:

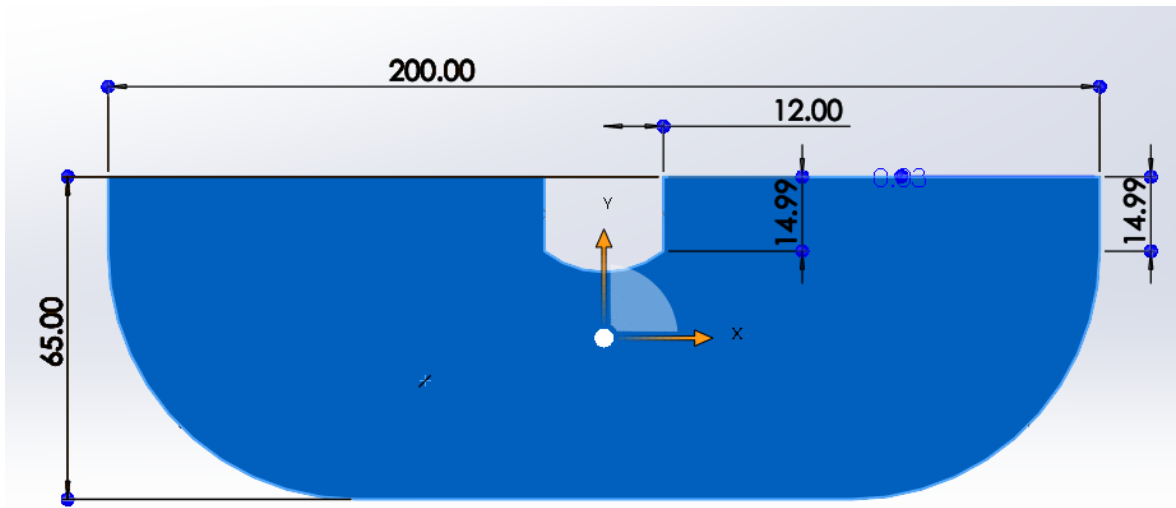


Figure 3.1: Wing Configuration for 20cm span

To adapt this wing configuration according to span of 60cm, the above-mentioned dimensions were scaled up to 3 times keeping the aspect ratio same. The final wing configuration for the wingspan of 60cm with aspect ratio of 3.50 is as follows:

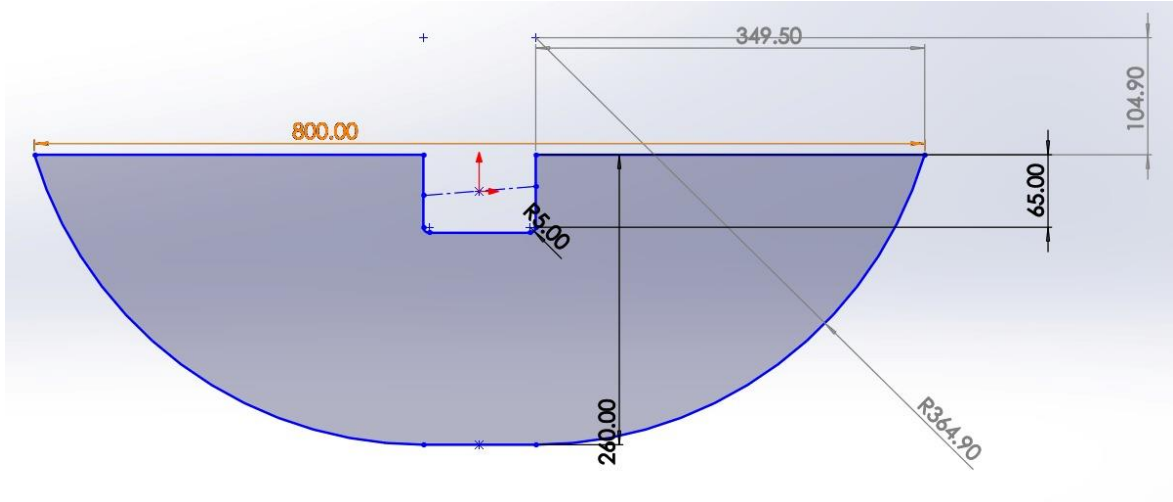


Figure 3.2: Wing Configuration for 80cm span

3.6.2 Wing Skeleton:

The first selected wing skeleton was of 20cm span wing. But the main problem with this skeleton is that it is for 20cm span but our required wingspan is 60cm. As the span increases, the no of skeleton rods and shape changes respectively. So, another wing skeleton of 88.5cm span was selected just to be on safe side. Both skeletons are given below in the following figure:

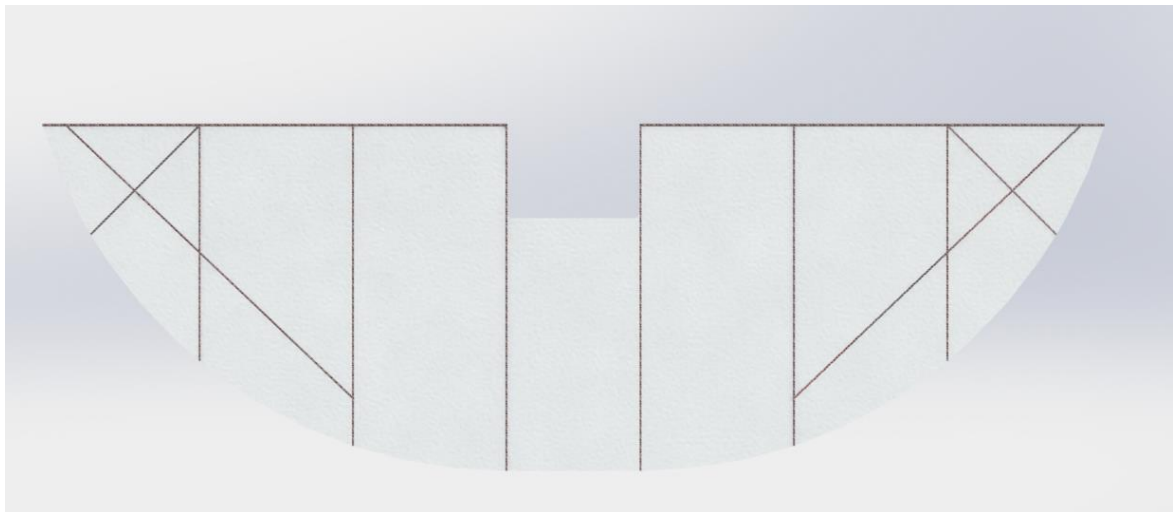


Figure 3.3: Wing Skeleton for 80cm span

To choose which skeleton is going to be in our final design, it is decided to test both skeletons in our final wing design and then select the one based on results.

3.6.3 Wing Skeleton Material:

It is important to choose a material with high rigidity, long durability, low weight, strong chemical resistance, heat tolerance, and low thermal expansion. Over steel and aluminum, carbon fiber was selected as the material for the wing frame to meet all these requirements.

3.6.4 Wing Membrane Material:

The wing membrane material should be lightweight, flexible and at an equivalent time high shear strength. Based on that properties, the best possible materials are polyethylene (PE), Orcon and Parylene. Parylene is the best one in terms of weight and strength but it's coating is a time-consuming process and requires a proper parylene coating equipment. Furthermore, polyethylene (PE) is not easily available in the market. So, Orcon is selected as our final wing membrane material.

3.7 Fuselage:

The fuselage of an ornithopter can be broken down into two parts: skeleton and body. Skeleton is the inner structure that is responsible for holding all the electronics, the mechanism in the front, and the tail end of the aircraft. Whereas the body is the enveloping structure that gives the robot semblance of a bird and reduce drag on the body.

3.7.1 Skeleton:

Special care must be exercised in the design of the skeleton as it should not take more mass than necessary; this helps in avoiding increase in total weight. The methodology for designing fuselage draws heavy inspiration from the world of DIY hobby RC fixed wing

aircrafts. Many tricks of the trade were applied here to obtain a robust structure while remaining frugal with weight. The skeleton comprises of carbon fiber rods, bridging the gap between mechanism base in the front and the plate supporting the tail at the rear. The plate supporting the tail is in the shape of a trapezoid and has holes to make it lean.

Starting with the length of the fuselage along its longitudinal axis, it was found that an ideal ratio is 75 percent of the span. As for the lateral length or thickness of the fuselage, it is controlled by the diameter of the available carbon fiber rod.

3.7.2 Body:

The body is a lightweight bird shaped Styrofoam structure that envelops the skeleton. It protects the aircraft during crashes, reduces overall drag—though not enough to justify its presence, and lastly, and most importantly given the purpose of the project, it gives the robot appearance of a bird.

3.8 Simulations

3.8.1 FEA Analysis of Gear Train:

The static structural analysis proved to be crucial in the design of gear train due to the fact that the gears were procured, and the specification sheet was absent. To incorporate the said gears in analysis, an accurate 3D model of the gears was engendered on SOLIDWORKS 3D CAD using the necessary measurement devices to measure the dimensions of the gear. Once a model was achieved with close tolerances it was put into the accompanying SOLIDWORKS Simulations software to determine the feasibility of the procured gears in our design.

The choice of SOLIDWORKS Simulations over other simulation software's was a simple one since the geometry was easy to import, modify, and assemble/disassemble in the SOLIDWORKS Simulations environment. Moreover, SOLIDWORKS Simulation had all the available modules that were needed to get a comprehensive look at the situation that was being analyzed.

To save time and computation cost, only first stage of the simple compounded gear train was analyzed; making the gear fixed and applying a torque and an angular displacement to the pinion—the figures for which were obtained using the procured motors specification sheet. Furthermore, the gear pinon contact was kept non penetrating to obtain indicative data and to have the option of introducing friction on the contact later.

3.8.2 FEA Analysis of Mechanism:

The transient analysis was done on Ansys 2022 R2 to see that the selected mechanism can sustain the torque and angular motion due to gears and motor, and the reaction forces due to wing flapping motion. As it is a transient analysis, the time steps are performed. The no of time steps and their details are as follows:

$$\textit{Number of Steps} = 1$$

$$\textit{Step End Time} = 2s$$

$$\textit{Auto Time Stepping} = \textit{OFF}$$

$$\textit{Time Step} = 1e^{-003}$$

Four revolute joints are attached to allow full motion to crank, connecting rod and rocker. A torque of 0.2381Nm and rotational velocity of 38rad is applied to the revolute joint of

crank attached with ground. Moreover, a vertical downward force of 0.5N is applied on rocker as an estimate of the reactions forces due of wing flapping motion.

3.8.3 CFD Analysis on wings:

CFD Analysis on the wings was done to calculate the pressure on the wing to select the right material which could withstand the pressure during up and down strokes of the flaps.

For this analysis SolidWorks model of the wing was imported in Ansys for transient analysis. Tetrahedral meshing was used with 50,236 mesh points.

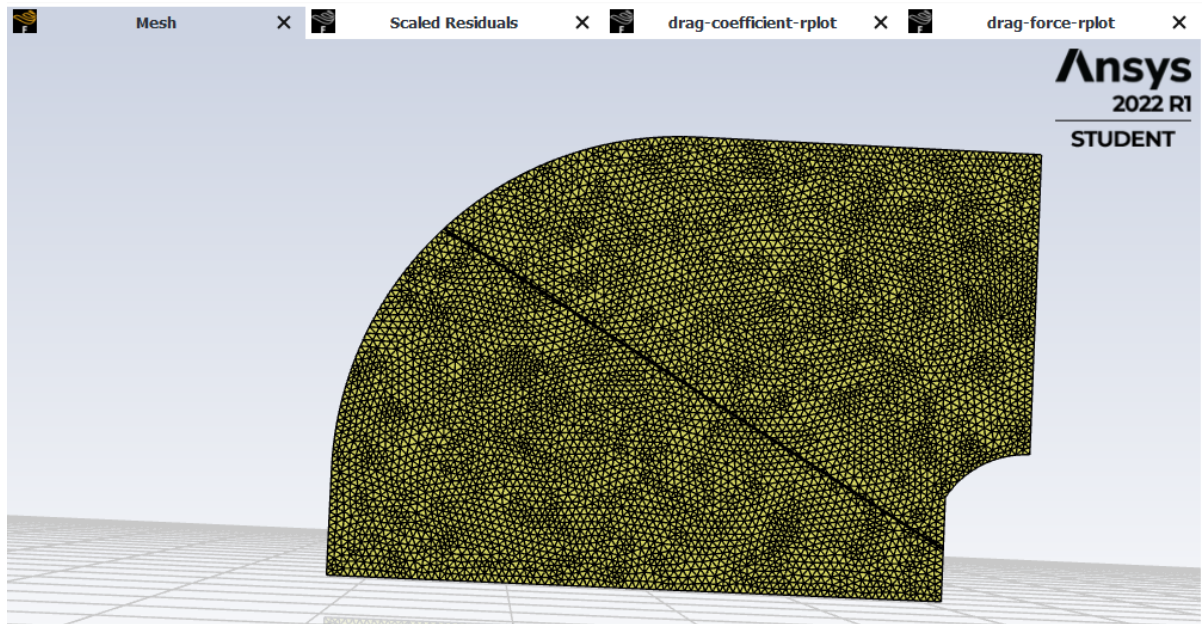


Figure 3.4: Wing Mesh

In aerodynamic applications, two models are commonly used: the Spalart Allmaras and k-omega models. However, it has been observed that the Spalart Allmaras model may lead to overestimation of turbulence production near the walls and is not suitable for high

strength flows. As a result, the Spalart Allmaras model can be utilized for the initial stage of solution to enhance convergence, but it cannot be used as the primary model for calculating fluid flow results. In contrast, the k-omega models are more effective in this regard, particularly the k-omega SST variation, which can efficiently calculate both near wall effects and core flow effects. Therefore, in this study, the k-omega SST model was utilized as the primary model for fluid flow calculations.

3.9 Final Testing:

Final Testing was done in a controlled environment in a stepwise manner. Followings were the methods of testing the working mechanism of the ornithopter:

3.9.1 Rudder and Elevator:

The Rudder and Elevator were assembled with the model and integrated with electronic circuit that is with flight controller, it was then tuned with the transmitter. The rudder and elevator were tested for different speeds and configurations thoroughly.

3.9.2 Stability testing:

The Ornithopter was tested for its stability with and without flapping the wings to avoid nosedives or any other instabilities during flight. It was done by hanging the ornithopter with a string to the roof. First CG was tested and then string was attached at that point to test the stability during flapping.



Figure 3.5: Final Model for Static Testing

3.9.3 Thrust Testing:

Thrust testing was done in a controlled environment by hanging the ornithopter with a rotatable platform with 100 cm radius. The ornithopter was flapped at different speeds and rudder and elevator angles to find variations of the thrust it can produce under all those conditions.

CHAPTER 4

RESULTS & CONCLUSIONS

4.1 Final Parameters:

Final design parameters after considering all the literature and going through the regress process of analysis and designing using analytical equations mentioned in the previous sections are as follows:

Table 4.1: Final Parameters

Parameter	Unit	Value
Permissible Mass	G	388
Wingspan	Cm	80
Required Frequency	Hz	3
Mass of Equipment	G	250
Gear Ratio		9.524
Battery Output	V	7.4
Motor ratings	Kv	1000
Total Flap Angle	degrees	55
Flight time	Min	5

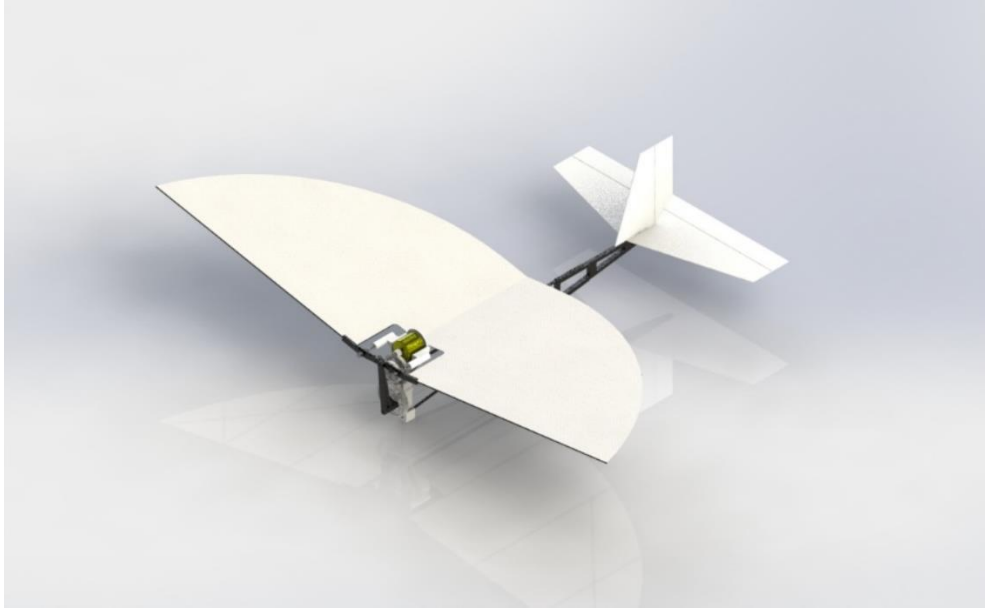


Figure 4.1: Rendered Final Model

4.2 Equipment selection:

The Equipment for the project was chosen using a methodology outlined in the corresponding chapter. The selection process took into account design considerations such as power requirements and weight limitations.

Following are the parameters of the equipment chosen for the design:

4.2.1 Motor:

<i>Name</i>	<i>A2212 1000KV Brushless DC Motor</i>
<i>Weight</i>	<i>50.5 g</i>
<i>ESC</i>	<i>30A Standard BLDC ESC (2-3 Cell LiPo)</i>



Figure 4.2: A2212 1000KV Brushless DC Motor

4.2.2 Servo Motor:

<i>Name</i>	<i>TowerPro SG90 Plastic gear servo</i>
<i>Weight</i>	<i>10 g</i>
<i>Torque</i>	<i>1.6 kg/cm</i>



Figure 4.3: TowerPro SG90 Plastic gear servo

4.2.3 Battery:

<i>Name</i>	<i>Lipo Battery</i>
<i>Weight</i>	<i>45 g</i>
<i>Discharge Rate</i>	<i>40 C</i>
<i>Capacity</i>	<i>850 mAh</i>
<i>No. of cells</i>	<i>2S</i>

4.2.4 Fuselage Material:

<i>Material</i>	<i>Carbon Fiber</i>
<i>Diameter</i>	<i>4mm</i>
<i>Length</i>	<i>45 cm</i>



Figure 4.4: 4mm carbon fiber

4.2.5 Mechanism:

<i>No. of Gears</i>	<i>4</i>
<i>Teeth on Gear 1</i>	<i>15</i>
<i>Teeth on Gear 2</i>	<i>80</i>
<i>Teeth on Gear 3</i>	<i>56</i>
<i>Teeth on Gear 4</i>	<i>100</i>
<i>Rocker arm</i>	<i>2.5 cm</i>
<i>Linkage length</i>	<i>6.8 cm</i>
<i>Crank Radii</i>	<i>1.15 cm</i>

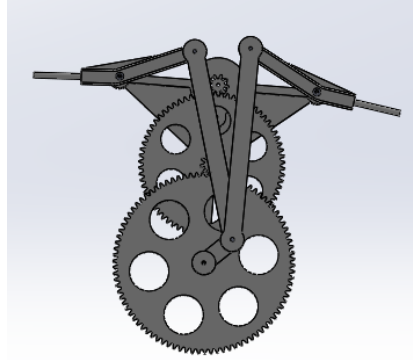


Figure 4.5: Gear Mechanism

4.2.6 Wings:

<i>Membrane Material</i>	<i>Orcon Paper</i>
<i>Skeleton Material</i>	<i>Carbon Fiber</i>
<i>Wings span</i>	<i>80 cm</i>
<i>Wings area</i>	<i>1525 cm²</i>

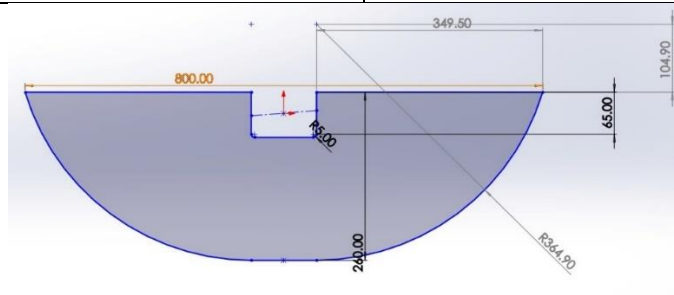


Figure 4.6: Wing Configuration with orcon paper

4.2.7 Tail:

<i>Material</i>	<i>Foam Board</i>
<i>Horizontal Stabilizer Span</i>	<i>35 cm</i>
<i>Vertical Stabilizer Span</i>	<i>12 cm</i>
<i>Total Tail Area</i>	<i>0.038827 m²</i>

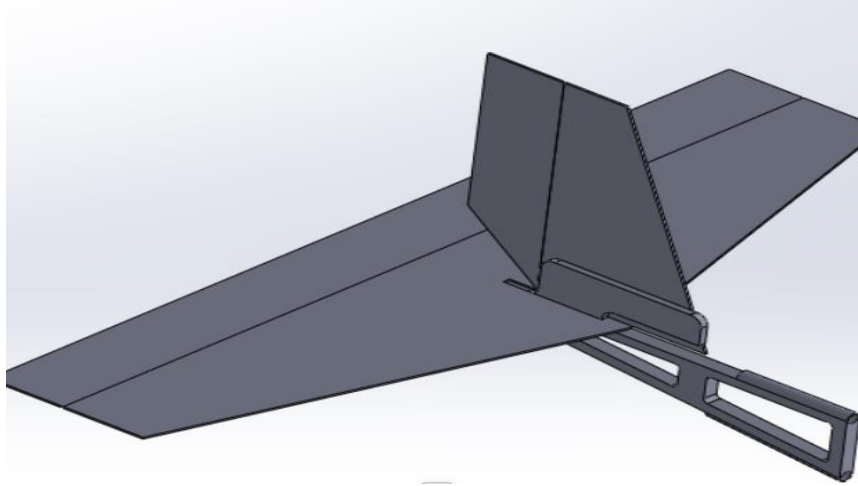


Figure 4.7: Tail Configuration with Foam Board

4.3 FEA Analysis:

FEA analysis was done to assure the quality of the mechanism and to assure that gear train could sustain the loads and drag force on the mechanism applied by the flapping of the wings. The analysis on separate parts of mechanism are as follows:

4.3.1 Structural Analysis of Gear Train

In any structural analysis, the most important factor that must be considered in the actual design is the von mises stress generated. It provides an accurate failure criterion to compare against.

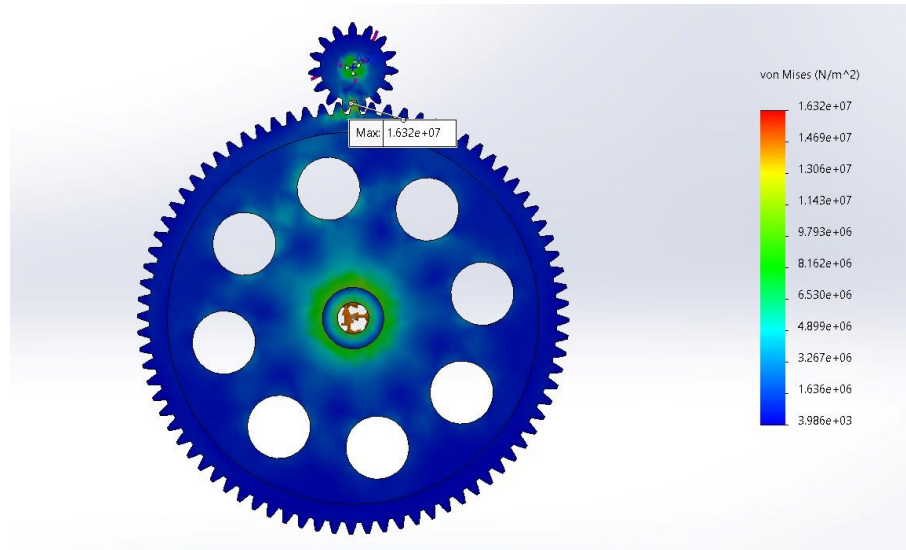


Figure 4.8: Von-Mises Stress for gear assembly

The following figure showcases the region where the highest von mises stress occurs. Although it was expected that the highest stress would be generated at the contact of gear pinion mesh, the values of the stresses is of special interest; these figures would be used in factor of safety calculation—incorporated due to the material of the gears.

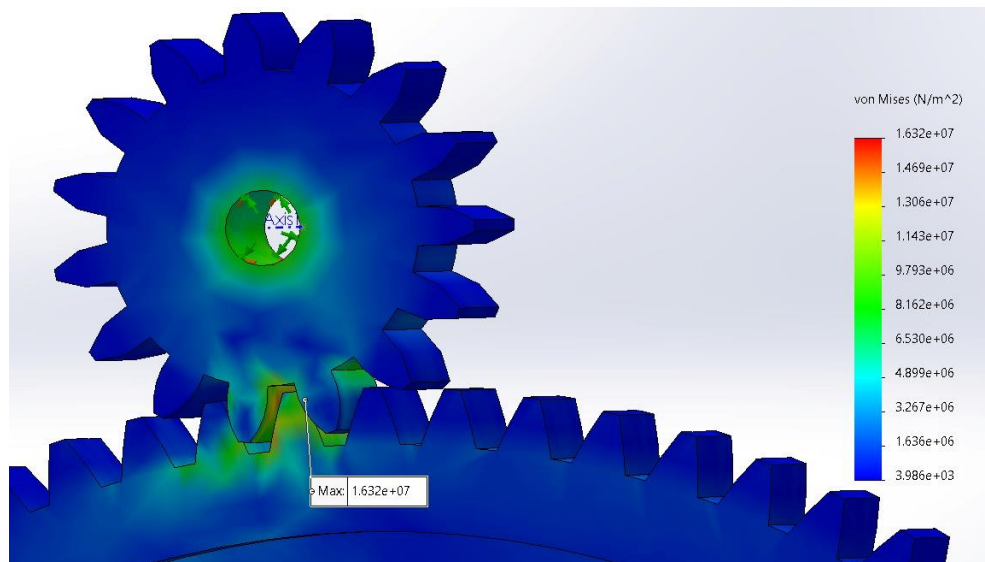


Figure 4.9: Zoomed version of Von-Mises Stress

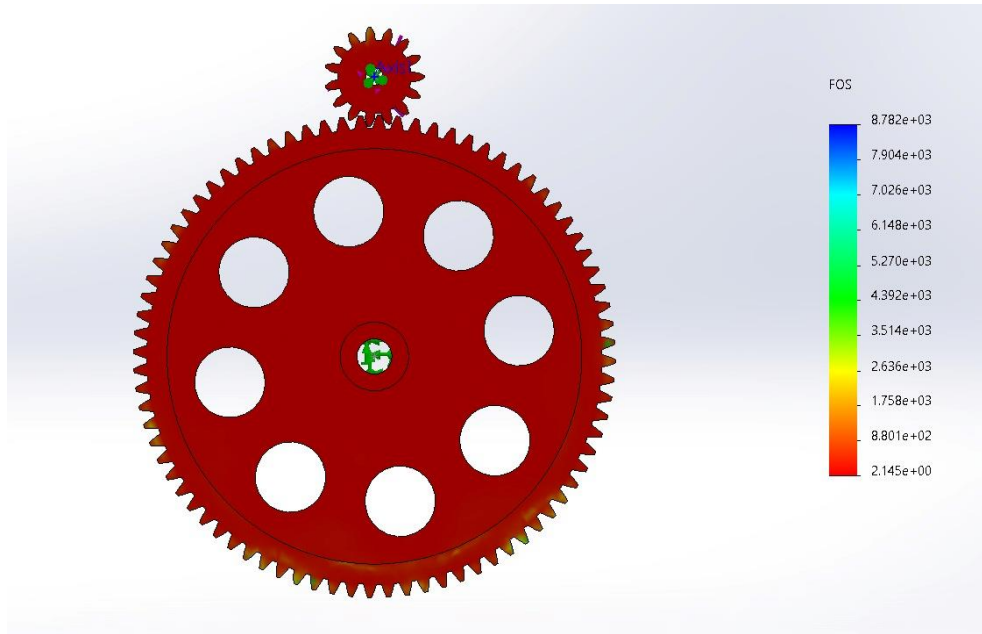


Figure 4.10: Factor of Safety analysis for Gear Assembly

4.3.2 Transient Analysis of Outboard Wing Hinge Mechanism:

The equivalent stress results of the simulation are as follows:

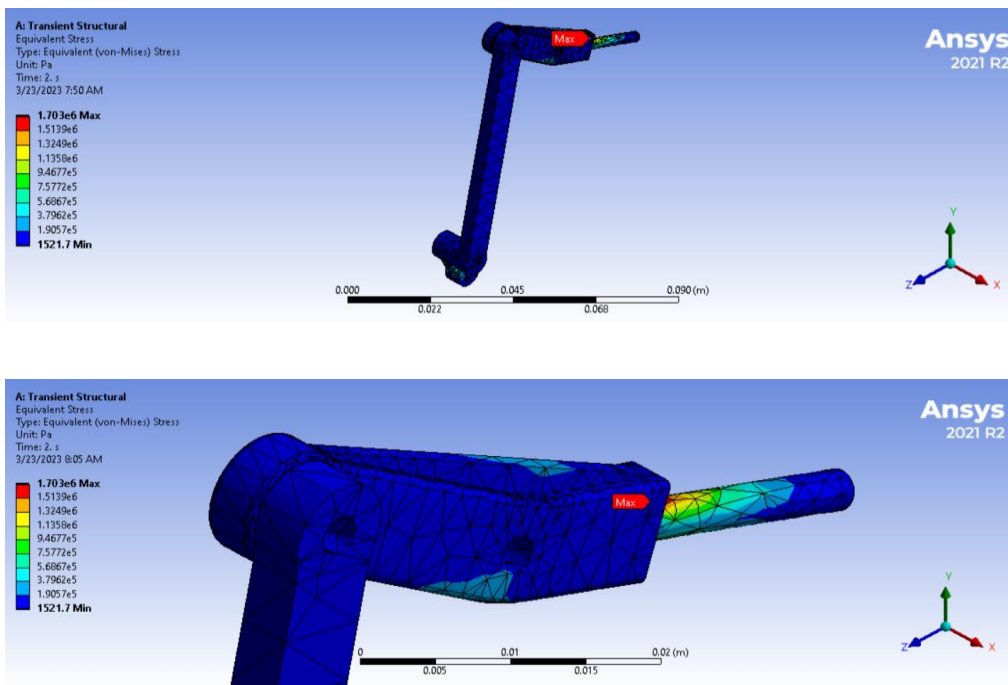


Figure 4.11: Equivalent Stress Analysis for Outboard Wing Hinge

It can be seen from above figures that the maximum stress is occurring at that part of rocker which is holding the wing spars. It was expected because this part of rocker is resisting the reaction forces of wing flaps. The maximum value of equivalent stress at the contour is showing 1.703×10^6 Pa. For this value, the calculated factor of safety is 30.24 with respect to yield strength of PETG material. It means that selected design is on safe side.

The deformation and the elastic strain contours are also shown in the following figures:

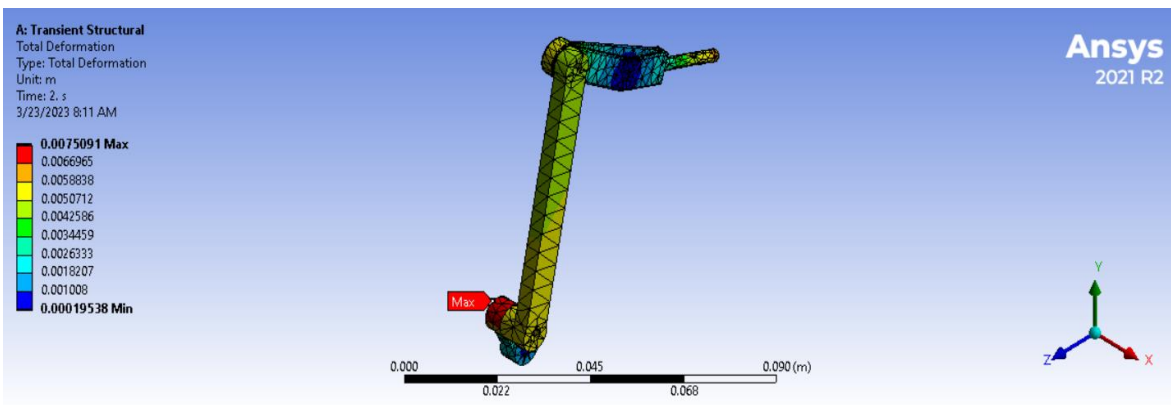


Figure 4.12: Total Deformation Analysis for Outboard Wing Hinge

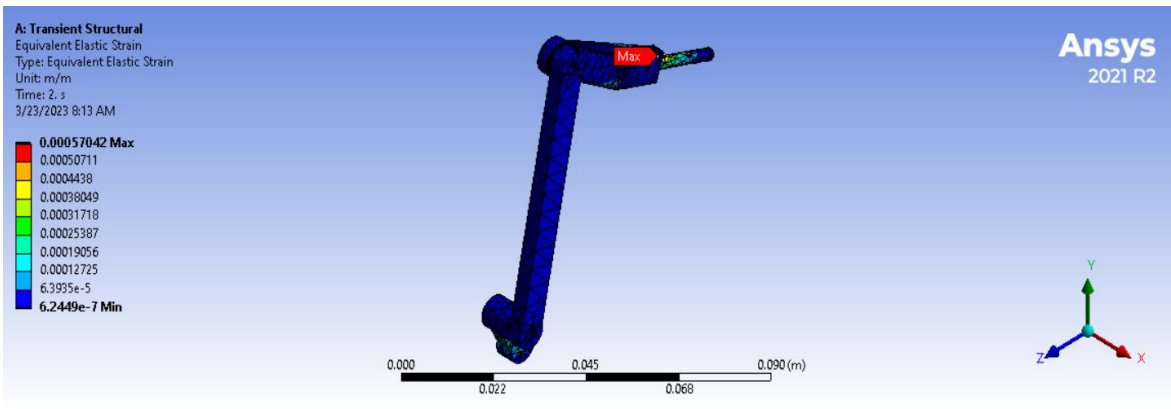


Figure 4.13: Equivalent Elastic Strain for Outboard Wing Hinge

From above figures, the maximum deformation of 0.0075091m is occurring at crank because of the applied torque and rotational velocity at its revolute joint. Moreover, the maximum strain is also occurring at rocker because this is the point of maximum stress concentration. And we know that strain is directly proportional to stress.

4.4 CFD Analysis:

The following results show that the maximum pressure is exerted on the leading edge of the wing where a carbon fiber rod is used to re-enforce the wing structure. The reason for this contour is high turbulence at the edges of the wings which create wakes and in turn high pressures areas are generated. While at the trailing edge the material is flexible to be bent, so the pressure is converted there to bend the membrane.

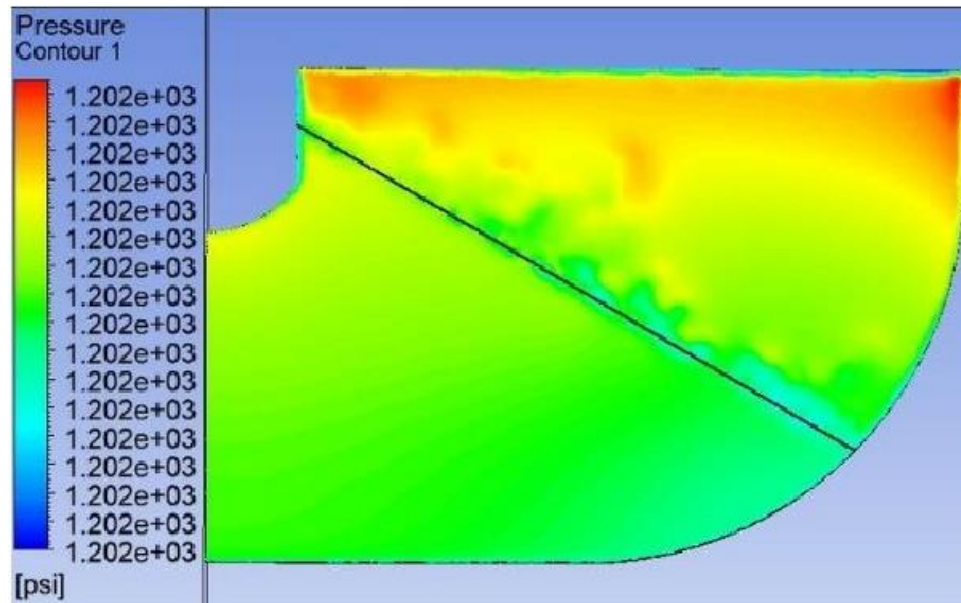


Figure 4.14: Pressure Distribution on Wing Membrane

The CFD analysis shows the pressure contour on the down stroke face of the wing which gives us the value of the pressure = 1202psi which is very low as compared to the yield strength of membrane (polyethylene) which is 3800psi.

4.5 Manufacturing Plan:

After the completion of the design and selection process for the required materials and components, the next steps in the manufacturing process involve procuring and 3D Printing of these materials of the final product.

4.5.1 Procurement:

Parts available in the market with better build quality in affordable price were procured these parts involve:

- DC Motor
- Servo motors
- Carbon fiber rods
- Gears
- Wings and tail material
- Fuselage outer body

4.5.2 3D Printing:

The material unavailable in the market in accordance with the design was 3D printed, these parts involve:

- Four bar linkages
- Flapping hinge

4.5.3 Assembly:

The assembly of the final product was carried out in the Aerial Robotics Lab, under the close supervision of a Lab Engineer who utilized advanced tools available in the lab to

ensure that the assembly process was defect-free. Prior to the assembly, all equipment was thoroughly tested in the lab to ensure the high quality of the final product.

4.5.4 Equipment Testing:

Upon the completion of the assembly process, all parameters were meticulously measured in the lab to guarantee the attainment of the desired output from all equipment. This involved measuring the flapping frequency, motor output, battery voltages, and servos.

4.5.5 Improvements:

The discrepancies between the calculated and actual results were addressed by revisiting the equipment and making necessary improvements to eliminate any potential ambiguities, and the process is repeated until the results matched, and we had a perfect machine to proceed for the flight tests.

4.6 Testing Results:

Testing of ornithopter was done according to above mentioned methodology and following results were concluded:

4.6.1 Rudder and Elevator:

After undergoing several failures and undergoing minor modifications, the rudder and elevator systems have been determined to function flawlessly. These findings demonstrate the successful outcome of the project.

4.6.2 Stability Testing:

CG was found at 15cm from the nose at central carbon fiber rod. It had perfectly stable test during flapping after few iterations of adjusting placement of electric components like battery and flight controller.

4.6.3 Thrust Testing:

The unavailability of a load cell and a thrust measuring apparatus made it impossible to quantify the amount of thrust the ornithopter was generating but a pretty good estimate could be made through the make shift apparatus. The ornithopter was capable of producing enough thrust to propel itself forward along with the platform it was tied to. This test assured that in actual flight the ornithopter will be able to push itself forward even against a small turbulence of air.

CHAPTER 5

CONCLUSION

In conclusion, our final year project on the design and implementation of a Flapping Wing Aerial Vehicle (FWAV) has demonstrated the feasibility of this unique type of aerial vehicle as a potential alternative to traditional aircraft for specific applications. Our prototype FWAV was designed and built using lightweight materials and tested in various flight conditions, showing stable flight performance with good maneuverability and agility.

The advantages of the FWAV design include improved maneuverability and agility, making it particularly useful in applications where traditional aircraft may not be effective. However, there are also some limitations to this design that need to be addressed before it can be widely adopted. These include the power source required to drive the flapping wings and the complexity of the design that requires precise control.

Future designs could incorporate more efficient power sources such as solar panels or fuel cells to overcome the limitation of battery-powered flight time and range. Autonomous control systems that use sensors and algorithms could also be incorporated to improve control precision and reduce reliance on skilled operators.

Overall, our project has provided valuable insights into the design and implementation of a FWAV, which has potential applications in various fields such as surveillance, environmental monitoring, and search and rescue operations. Further research is needed to address the limitations of this design, but our project has laid a solid foundation for future development in this exciting field of aviation.

References

- [1]. The Ornithopter Design Manual (Fifth Edition, Nathan Chronister, 2008)
- [2]. Development Scenario of Micro Ornithopters (Lung-Jieh Yang, Suseendar Marimuthu, Kuan-Cheng Hung, Hao-Hsiang Ke, Yow-Ting Lin and Chien-Wei Chen, December 2015).
- [3]. Design Development and Analysis of Ornithopters (Kushal Jadhav, Harshada Javheri, Nikita Durge, Akash Hange, Asst. Prof. Rohit R. Chavan, July 2020)
- [4]. Flapping Wing Vehicles Numerical and Experimental Approach (Lung-Jieh Yang, Balasubramanian Esakki, 2022)
- [5]. Ornithopter Type Flapping Wings for Autonomous Micro Aerial Vehicles (Sutthiphong Srigrarom, Woei-Leong Chan, May 2015)
- [6]. Design Guidelines for Flapping Wing Micro UAVs (Salman A. Ansari, Kevin Knowles and Rafał Żbikowski, 2005)
- [7] <https://github.com/OrnithopterX/Ornithopter-Crank-Designer> (Joshua Adcock, Wilford Willams)
- [8] = "Design and Implementation of Autonomous Flight Control System for Quadcopter using Arduino" by K. Adarsh et al. (2020)
- [9] = "Design and Optimization of a Brushless DC Motor for UAV Propulsion Systems" by M. K. Ali, M. A. Hannan, M. R. Islam, and A. Mohamed
- [10] = "Evaluation of Li-ion Battery Chemistries for Small Unmanned Aerial Vehicles" by J. G. Simpson, R. Mohan, and M. Pecht.
- [11] = "A Method for Designing V-Tails," by Daniel Raymer.

[12] = "Fuselage Aerodynamics and Weight Trade-Off at Low-Speed Ornithopter Flight"
published in the IEEE (Institute of Electrical and Electronics Engineers)

Annexure A

